ChemComm

Evaluation of the role of DNA surface for enhancing the activity of scaffolded enzyme

Journal:	*ChemComm*
Manuscript ID	CC-COM-01-2021-000276.R1
Article Type:	Communication

COMMUNICATION

Evaluation of the role of DNA surface for enhancing the activity of scaffolded enzymes†

Received 00th January 20xx,
Accepted 00th January 20xx

DOI: 10.1039/x0xx00000x

Peng Lin,[a] Huyen Dinh,[a] Yuki Morita,[a] Zhengxiao Zhang,[a] Eiji Nakata,[a] Masahiro Kinoshita[a] and Takashi Morii*[a]

The catalytic enhancements of enzymes loaded on DNA nanostructures have been attributed to the characteristics provided by highly negative charges on the surface of scaffold, such as modulation of the local pH near enzyme. In this study, two types of enzyme with the optimal activity at pH 6 or 8 equally displayed significant catalytic enhancements on the DNA scaffold. By using a ratiometric pH indicator, a lower local pH shift of 0.8 was observed near the DNA scaffold. The postulated local pH change near the DNA scaffold surface unlikely plays a general role in enhancing the activity of scaffolded enzymes.

Enzymes have been widely applied in the fields of chemical, medical and food industries.[1] Immobilizing the enzymes of interest on the surface of carrier provides the simplest yet useful method for practical enzyme applications.[2] Immobilized enzymes often display higher activity and stability than the free form, however, the exact mechanism for the enhanced activity is still under debate.[3] Enhancement of the stability and/or catalytic activity of immobilized enzymes were observed for a broad range of carriers, such as protein, lipid, silica, graphene oxide, polymers and DNA-based materials.[4] Understanding the origin of enhanced activity of immobilized enzymes accelerate the logical design of effective catalysts.

Among the carriers for immobilizing enzymes, DNA scaffolds, such as DNA origami, attract great interest as enzyme templates by the structural programmability and accurate addressability.[5] A series of individual- or multi-enzyme systems have been located on DNA structures with control over the positions and stoichiometry of enzymes.[6] While these studies illustrate increasing yields of coupled enzyme reactions, enhanced activities of single type of DNA scaffolded enzymes have been reported.[7] Several mechanisms were proposed to describe the increased catalytic ability. Compared to the other enzyme carriers, high, negative surface charge density is a distinctive character of DNA nanostructures. It was hypothesized to form the ordered hydration layer that contributed to the catalytic enhancement by stabilizing the structure of enzyme[7a] or the micro-environment that increased catalytic activity without modifying the affinity of enzyme for the substrate.[7b] Furthermore, the catalytic enhancement of DNA scaffolded enzymes could be caused by more general factor like reduction of the adsorption on the reaction vessels.[7c] It was also suggested that substrates were attracted to the negatively charged surface of DNA nanostructure through electrostatic interaction, leading to the enrichment of substrates near the surface and enzymes.[8] Besides these factors, modulation of the local pH environment by the highly negative charges on DNA scaffold surface was proposed as a critical element to increase enzyme activity on DNA scaffold.[9] However, such a local pH change could limit the general application of DNA nanostructures for scaffolding enzymes because the enzymes are built up with their own optimal pH preferences. The relevance to the local pH environment of DNA scaffold could be limited to a few enzymes tested so far, which exhibited the similar pH dependence with an increased maximal turnover rate in more acidic conditions.[9]

In this study, two enzymes with different pH preferences, xylose reductase (XR) and xylitol dehydrogenase (XDH), were individually assembled on DNA scaffold[10] through the modular adaptor.[11] The catalytic enhancements were observed for both the scaffolded XR and XDH over the respective free enzyme (Fig. 1). The different optimal pH profiles of XR (pH 6.0) and XDH (pH 8.0), the neutral or net negative charge of their substrates and cofactors indicated that neither the local pH change nor the surface-substrate or -cofactor electrostatic attractive interaction accounted for the increase in activities of assembled enzymes. We also suggest that improved stability or reduced adsorption of scaffolded enzymes alone is not the determining factor for enhancing the activity of enzyme on DNA scaffold.

A square pyramidal DNA scaffold derived from the open state of DNA robot[10] was constructed by DNA origami (Fig. S1 and S2, ESI†). The scaffold consisted of two boat forms that were covalently attached in the rear by single-stranded scaffold

[a] Institute of Advanced Energy, Kyoto University, Uji, Kyoto 611-0011, Japan. Email: t-morii@iae.kyoto-u.ac.jp

† Electronic Supplementary Information (ESI) available. See DOI: 10.1039/x0xx00000x

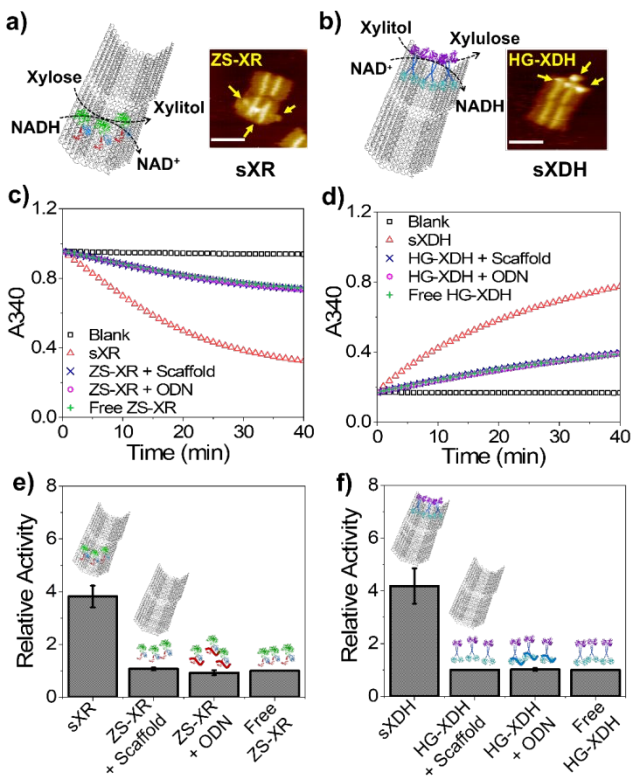

Fig. 1 (a) ZS-XR assembled on the DNA scaffold (sXR) and its AFM image, scale bar: 100 nm. (b) HG-XDH assembled on the DNA scaffold (sXDH) and its AFM image, scale bar: 100 nm. (c) Time course of ZS-XR reactions monitored by the absorbance at 340 nm (A340). (d) Time course of the HG-XDH reactions monitored by A340. (e) Relative activities of sXR and free ZS-XR. (f) Relative activities of sXDH and free HG-XDH. All the reactions were carried out with enzyme concentrations of 5 nM.

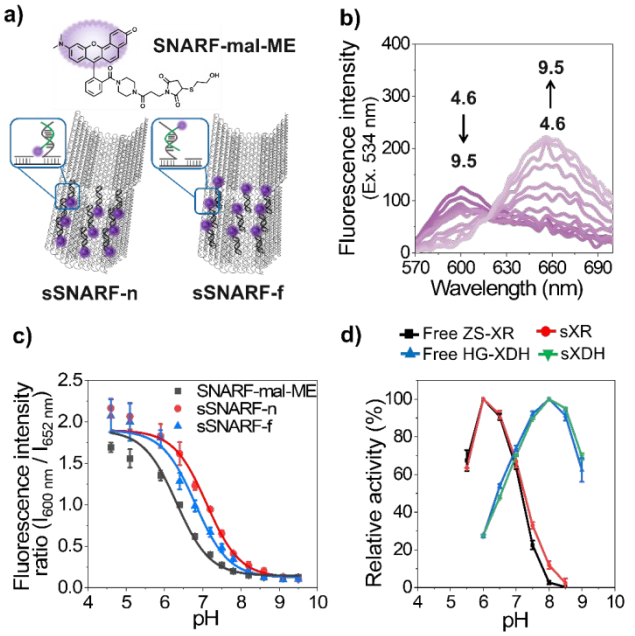

Fig. 2 (a) Structures of SNARF-mal-ME (top), SNARF facing near DNA scaffold surface (sSNARF-n, bottom left), SNARF locating 6.7 nm far apart from the surface (sSNARF-f, bottom right). (b) Fluorescence emission spectra of sSNARF-n upon excitation at 534 nm in the buffer ranging from pH 4.6 to 9.5. (c) Titration of the fluorescence intensity ratio (I_{600} / I_{652}) against the solution pH. (d) The pH profiles for relative activity of enzymes in free form and assembled on the DNA scaffold, here the pH indicates the buffer pH.

hinges (Fig. S3, S4, S5 and S6, ESI†). The carbohydrate substrate for each enzyme, xylose for XR or xylitol for XDH, bears no charge, and the cofactor for each enzyme, NADH for XR or NAD^+ for XDH, shares net negative charge near the neutral pH. A modular adaptor fused enzyme XR (ZS-XR) was constructed and loaded on the DNA scaffold through the covalent linkage as reported previously.[11b] Xylitol dehydrogenase (XDH)[12] was fused to the C-terminal of modular adaptor HG consisting of the basic leucine zipper protein GCN4[13] and the Halo-tag[14] to construct enzyme HG-XDH. The Halo-tag substrate 5-chlorohexane (CH) was incorporated near the GCN4-binding DNA sequence (Fig. S7 and S8, ESI†). DNA scaffold was designed with three binding sites modified with BG for ZS-XR or those with CH for HG-XDH (Table S1, ESI†). Loading yield of ZS-XR or HG-XDH on the DNA scaffold quantitated from AFM images[15] was 2.5 molecules of monomer or 2.5 molecules of dimer on each scaffold, respectively (Fig. 1a, 1b, S9, S10, Table S2 and Note S1, ESI†).

The reaction of XR or XDH at pH 7.0 was analyzed by monitoring the consumption or production of NADH spectrophotometrically at 340 nm. The turnover frequency of scaffolded ZS-XR (sXR) was almost 4-fold higher than free ZS-XR in the presence of DNA scaffold without its binding sites (ZS-XR + Scaffold), ZS-XR modified with a BG modified oligodeoxyribonucleotide (ZS-XR + ODN), or free ZS-XR (Free ZS-XR) (Fig. 1c, 1e and S11, ESI†). The turnover frequency of scaffolded HG-XDH (sXDH) was also increased by over 4 times than free HG-XDH in the presence of DNA scaffold without its binding sites (HG-XDH + Scaffold), HG-XDH modified with a CH modified ODN (HG-XDH + ODN), or free HG-XDH (Free HG-XDH) (Fig. 1d, 1f and S12, ESI†). The catalytic enhancements were observed for both scaffolded enzymes. To assess the local pH environment of DNA scaffold, a dual-emission ratiometric pH indicator SNARF derivative[16] was loaded on the DNA scaffold either facing near the surface (sSNARF-n) or locating 6.7 nm away from the surface (sSNARF-f), which roughly corresponded to the distance between enzyme and surface of DNA scaffold (Fig. 2a and S2, Table S3 and S4, ESI†). The maleimide-attached SNARF derivative modified by mercaptoethanol (SNARF-mal-ME) (Fig. 2a, top) was utilized as a standard. Upon excitation at 534 nm, the spectra exhibited fluorescence emission peaks at 600 nm and 652 nm. As the pH of the solution increased from 4.6 to 9.5, emission intensities at 600 nm decreased, whereas that at 652 nm increased (Fig. 2b and S13, ESI†). The ratio of fluorescence intensity at 600 nm over 652 nm was plotted against the buffer pH to deduce pH titration curves (Fig. 2c and S13, ESI†). The pK_a values of SNARF-mal-ME, sSNARF-n and sSNARF-f were 6.3 ± 0.1, 7.1 ± 0.1 and 6.8 ± 0.1, respectively (Note S2, ESI†). The pK_a value of SNARF derivative shifted higher by 0.8 near the surface or 0.5 at 6.7 nm away from the surface. By using the titration curve of SNARF-mal-ME as the standard of bulk buffered solution, local pH near the surface or near the enzyme loaded position in the reaction buffer (pH 7.0) was deduced to be 6.2 and 6.5, respectively (Note S2, ESI†). The lower local pH might derive from the large and negatively charged surface of DNA scaffold which attracts the protons.[9a]

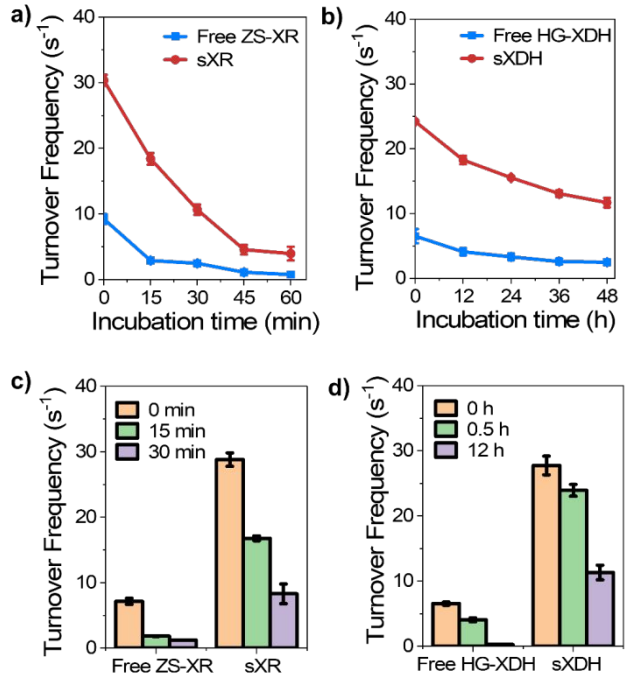

Fig. 3 Turnover frequencies of (a) free ZS-XR and sXR, and (b) free HG-XDH and sXDH after the indicated incubation time with BSA. Turnover frequencies of (c) free ZS-XR and sXR, and (d) free HG-XDH and sXDH after the indicated incubation time without BSA. All the reactions were carried out with enzyme concentrations of 2.5 nM.

The relative activity of free and scaffolded enzymes displayed almost identical pH profiles (Fig. 2d, S14 and S15, ESI†). Free ZS-XR and sXR showed the optimal activity at pH 6.0. Similarly, both free HG-XDH and sXDH displayed the optima at pH 8.0. Based on these pH profiles of enzyme activity, the local pH near the enzyme would result at most 25% enhancement of the catalytic activity for sXR and 30% reduction for sXDH (Fig. 2d). Therefore, the postulated modulation of enzyme activity by the lower pH shift near DNA scaffold surface[9a] unlikely explains the catalytic enhancements of both scaffolded enzymes (Fig. 1).

We next investigated the residual activity of scaffolded enzyme after incubation at ambient temperature to ask whether the enzyme was stabilized by scaffolding.[7a] After 15 min, remaining activities evaluated by the turnover frequency of free ZS-XR and sXR were 32% and 60%, respectively. Even considering the instability of free ZS-XR,[17] the tolerance of sXR against deactivation after the pre-incubation is not the sole determinant for the higher activity of sXR over free ZS-XR (Fig. 3a and S16, ESI†). sXDH also showed higher residual activity under the same conditions with the remaining activity of free HG-XDH and sXDH being 63% and 75%, respectively, after 12 h incubation (Fig. 3b and S17, ESI†).

The higher residual activity of scaffolded enzyme can be attributed to the prevention of adsorption of enzymes on the tube surface,[7c] as found in the case where BSA is added to the aqueous solution.[18] All the above enzyme reactions were evaluated in the presence of 5 μM BSA (Fig. 1c, 1d, 3a and 3b) because BSA was effective on retaining the activity of free HG-XDH in a concentration dependent manner up to 5 μM (Fig. S18, ESI†). To test whether the DNA scaffold could also prevent the enzyme deactivation, both the free and scaffolded enzymes were pre-incubated in the absence of BSA before starting reactions (Fig. 3c, 3d, S19 and S20, ESI†). Free ZS-XR and sXR incubated for 30 min without BSA retained 17% and 30%, respectively, of the original activity (Fig. 3c and S19, ESI†). Free HG-XDH and sXDH incubated for 30 min without BSA likewise retained 62% and 86%, respectively, of its original activity. After 12 h, HG-XDH almost completely lost the activity, while sXDH retained 40% of its original activity (Fig. 3d and S20, ESI†). The scaffold with high DNA helix packing density further protected the embedded enzyme against adsorption or deactivation even in the presence of BSA (Fig. 3a and 3b). The ordered hydration layer formed by negatively charged DNA scaffold surface was suggested to stabilize the enzyme configuration.[7a] In the case of HG-XDH, the dimeric form of XDH could be further stabilized upon binding the specific DNA sequence on the scaffold. However, the stabilizing effect alone cannot explain the 4-fold higher catalytic activity of scaffolded enzymes over the free enzymes.

Our results indicated that the local pH change modulated by the highly negative charges on DNA scaffold surface is not the general factor to enhance the activity of scaffolded enzymes, ensuring that DNA nanostructures are applicable to the scaffolding of many types of enzymes. The DNA surface-substrate electrostatic attractive interaction unlikely plays a dominant role in the present system for enhancing the catalytic activity of enzymes on DNA nanostructures because neither the substrate nor the cofactor possesses a positive net charge. On the other hand, the preserved stability and the prevention of adsorption of DNA scaffolded enzyme could partly contribute to the catalytic enhancement, but these effects alone are insufficient to explain the observed high activity of scaffolded enzyme. Therefore, contribution of the interaction between DNA carrier surface and enzyme must be considered further. It has been shown that a layer of water, whose density and orientational structures are substantially different from those of bulk water, is formed near a surface emanating strong electric field like the DNA surface.[19] The formation of this hydration layer is a plausible candidate for the general factor to enhance the catalytic activity of the enzyme scaffolded on DNA nanostructure. However, the correlation between the hydration layer and the enhanced enzyme activity is quite elusive. We have recently suggested that a hydrophobic substrate or cofactor is enriched within the domain confined between two enzyme surfaces due to the entropic force by water, leading to the enhancement of catalytic activity of packed enzymes over dispersed enzymes.[20] The mechanism of the activity enhancement in the present system, where the substrates are highly hydrophilic and the enzymes are near the DNA nanostructure, can be substantially different. A consideration based on statistical-mechanical theory of hydration as well as a series of systemized experiments is necessitated for elucidating the mechanism. Work in this direction is in progress at our laboratory.

This work was supported by JSPS KAKENHI Grant Numbers 17H01213 (T.M.) and 19H04653 (E.N.), and by JST CREST Grant

Number JPMJCR18H5 (T.M.), Japan. TEM measurement in this work was supported by Kyoto University Nano Technology Hub in "Nanotechnology Platform Project" sponsored by MEXT, Japan. Peng Lin would like to acknowledge the China Scholarship Council (CSC) for the PhD scholarship.

Conflicts of interest

There are no conflicts to declare.

Notes and references

1 R. DiCosimo, J. McAuliffe, A. J. Poulose and G. Bohlmann, *Chem. Soc. Rev.*, 2013, **42**, 6437-6474.

2 R. A. Sheldon, *Adv. Synth. Catal.*, 2007, **349**, 1289-1307.

3 Y. Zhang, J. Ge and Z. Liu, *ACS Catal.*, 2015, **5**, 4503-4513.

4 (a) S. Lim, G. A. Jung, D. J. Glover and D. S. Clark, *Small*, 2019, **15**, 1805558; (b) S. R. Tabaei, M. Rabe, H. Zetterberg, V. P. Zhdanov and F. Höök, *J. Am. Chem. Soc.*, 2013, **135**, 14151-14158; (c) Y. Wang and F. Caruso, *Chem. Mater.*, 2005, **17**, 953-961; (d) P. Lin, Y. Zhang, H. Ren, Y. Wang, S. Wang and B. Fang, *Eng. Life Sci.*, 2018, **18**, 326-333; (e) J. J. Virgen-Ortíz, J. C. dos Santos, Á. Berenguer-Murcia, O. Barbosa, R. C. Rodrigues and R. Fernandez-Lafuente, *J. Mater. Chem. B*, 2017, **5**, 7461-7490; (f) A. Rajendran, E. Nakata, S. Nakano and T. Morii, *ChemBioChem*, 2017, **18**, 696-716.

5 (a) P. W. K. Rothemund, *Nature*, 2006, **440**, 297-302; (b) S. M. Douglas, H. Detz, T. Liedl, B. Högberg, F. Graf and W. M. Shih, *Nature*, 2009, **459**, 414-418.

6 (a) G. Grossi, M. D. E. Jepsen, J. Kjems and E. S. Andersen, *Nat. Commun.*, 2017, **8**, 1-8; (b) O. I. Wilner, Y. Weizmann, R. Gill, O. Lioubashevski, R. Freeman and I. Willner, *Nat. Nanotechnol.*, 2009, **4**, 249-254; (c) T. A. Ngo, H. Dinh, T. M. Nguyen, F. F. Liew, E. Nakata and T. Morii, *Chem. Commun.*, 2019, **55**, 12428-12446.

7 (a) Z. Zhao, J. Fu, S. Dhakal, A. Johnson-Buck, M. Liu, T. Zhang, N. W. Woodbury, Y. Liu, N. G. Walter and H. Yan, *Nat. Commun.*, 2016, **7**, 1-9; (b) S. Rudiuk, A. Venancio-Marques and D. Baigl, *Angew. Chem., Int. Ed.*, 2012, **124**, 12866-12870; (c) C. Timm, C. M. Niemeyer, *Angew. Chem., Int. Ed.*, 2015, **54**, 6745-6750.

8 J. L. Lin and I. Wheeldon, *ACS Catal.*, 2013, **3**, 560-564.

9 (a) Y. Zhang, S. Tsitkov and H. Hess, *Nat. Commun.*, 2016, **7**, 1-9; (b) Y. Xiong, J. Huang, S. T. Wang, S. Zafar and O. Gang, *ACS Nano*, 2020, **14**, 14646-14654.

10 S. M. Douglas, I. Bachelet and G. M. Church, *Science*, 2012, **335**, 831-834.

11 (a) E. Nakata, H. Dinh, T. A. Ngo, M. Saimura and T. Morii, *Chem. Commun.*, 2015, **51**, 1016-1019; (b) T. A. Ngo, E. Nakata, M. Saimura and T. Morii, *J. Am. Chem. Soc.*, 2016, **138**, 3012-3021; (c) T. M. Nguyen, E. Nakata, M. Saimura, H. Dinh and T. Morii, *J. Am. Chem. Soc.*, 2017, **139**, 8487-8496.

12 S. Watanabe, T. Kodaki and K. Makino, *J. Biol. Chem.*, 2005, **280**, 10340-10349.

13 T. E. Ellenberger, C. J. Brandl, K. Struhl and S. C. Harrison, *Cell*, 1992, **71**, 1223-1237.

14 C. G. England, H. Luo and W. Cai, *Bioconjug. Chem.*, 2015, **26**, 975-986.

15 E. Nakata, H. Dinh, T. M. Nguyen and T. Morii, *Methods in Enzymol.*, 2019, **617**, 287-322.

16 (a) J. E. Whitaker, R. P. Haugland and F. G. Prendergast, *Anal. Biochem.*, 1991, **194**, 330-344; (b) E. Nakata, Y. Yukimachi, Y. Nazumi, Y. Uto, H. Maezawa, T. Hashimoto, Y. Okamoto and H. Hori, *Chem. Commun.*, 2010, **46**, 3526-3528.

17 S. Watanabe, A. A. Saleh, S. P. Pack, N. Annaluru, T. Kodaki and K. Makino, *Microbiology*, 2007, **153**, 3044-3054.

18 (a) T. Eriksson, J. Börjesson and F. Tjerneld, *Enzyme Microb. Technol.*, 2002, **31**, 353-364; (b) B. Yang and C. E. Wyman, *Biotechol. Bioeng.*, 2006, **94**, 611-617.

19 (a) G. M. Torrie, P. G. Kusalik and G. N. Patey, *J. Chem. Phys.*, 1988, **88**, 7826-7840; (b) D. R. Bérard, M. Kinoshita, N. M. Cann and G. N. Patey, *J. Chem. Phys.*, 1997, **107**, 4719-4728; (c) M. Kinoshita, *J. Sol. Chem.*, 2004, **33**, 661-687.

20 H. Dinh, E. Nakata, K. Mutsuda-Zapater, M. Saimura, M. Kinoshita and T. Morii, *Chem. Sci.*, 2020, **11**, 9088-9100.